Influence of the annealing temperature on $Ge_1Sb_2Te_4$ thin film prepared by pulsed laser deposition

M. JIGAU, M. OSIAC*, G. E. IACOBESCU
University of Craiova, Department of Physics, Street A.I. Cuza no. 13, Craiova 200585, Romania

In this study the $Ge_1Sb_2Te_4$ thin film has been deposited by pulsed laser deposition. The X-ray diffraction (XRD) was applied to show crystallization as deposited and annealed films. The change of film roughness and the topography of annealed films have been determined by Atomic Force Microscopy (AFM). The phonon modes of film were identified using Raman spectroscopy. It was observed that while increasing the temperature, the modes of vibration in the Raman spectra became more clearly defined, indicating good film crystallization. The qualitative chemical composition of $Ge_1Sb_2Te_4$ thin film measured by EDX presented the stoichiometry of thin film.

(Received August 17, 2016; accepted June 7, 2017)

Keywords: Pulsed laser deposition, Thin film, Chalcogenide GeSbTe

1. Introduction

It is well known that the phase change memory, the phase change optical disks used as a storage data especially for computers due to their high storage density, are represented by the Ge-Sb-Te materials. The phase-change memory uses fast and reversible change in the electrical resistivity between amorphous and crystalline phases. By using current pulses with different widths and heights, two states are possible; a short pulse switch to amorphous phase and the annealing effect is done by long pulse that switch to conductive crystalline state. The data storage density of optical disks is determined by the focused spot size of the laser beam used to write and read the data bits [1-4].

Recently, the chalcogenide thin film based on Ge-Sb-Te has been employed for phase change optical memories, for memory devices such as DRAM, SRAM and flash memory [5, 6]. The phase-change random access memory (PC-RAM) based on chalcogenide materials is regarded to be one of promising memories due to their properties as non-volatility, high speed, lower power, high-quality endurance for repetitious writing and alternative conventional CMOS based memory [7, 8]. Chalcogenide materials based on GeSbTe (GST) are used as active layers of optical memory discs (DVD), being under intensive research in order to develop alternative types of memories Phase-Change RAM (PC-RAM) or Chalcogenide RAM (C-RAM) to commercially successful semiconductor FLASH memories [8]. Optical and electrical data recording are based on reversible phase transformation between amorphous and crystalline phases [9], caused by laser or electrical pulses application. Detection of the data is based on contrast in reflectivity/resistance between amorphous and crystalline states. The GST thin films are finding application in electronics for data storage media including future non-volatile memories [10-14] and thermoelectric energy conversion [15]. The GST film can be deposited by various methods, as radio frequency and DC magnetron sputtering [16], metal organic chemical vapour deposition, thermal evaporation [17], high power impulse magnetron sputtering HiPIMS [18], and by pulsed laser deposition (PLD) [19-22].

In this paper, PLD method was used for the chalcogenide deposition, since it is a simple and easy process to control, with a high deposition rate and offers stoichiometric transfer from the target material to the thin films. The film characterization is done by atomic force microscopy AFM, energy dispersive X-ray analysis (EDX), X-ray diffraction (XRD) and Raman scattering spectroscopy.

2. Experimental

In this research, the PLD technique was used for $Ge_1Sb_2Te_4$ (GST-124) thin films preparation. This technique has been widely used for the deposition of various complex oxides and chalcogenide films. In PLD technique, a number of parameters such as growth temperature, pressure, laser fluency, laser spot area, and target-substrate distance can be easily adjusted to achieve the desired film properties [19-22]. The PLD set-up consisted of a vacuum chamber pump down until it reached the pressure of $p = 1.4x10^{-5}$Torr. The optical laser system is a Nd:YAG laser working on the second harmonic wavelength of 532nm with constant output energy of 110 mJ/pulse, pulse duration 10 ns and repetition rate 10 Hz. Energy density of the laser beam on the target surface was 0.4 Jcm^{-2}. The fluence value was taken so small in order to obtain amorphous thin film during deposition process. The laser beam hit the bulk chalcogenide GST-124 target to an angle of 45°. Target

was rotated to avoid crater formation, the distance target-substrate was kept constant at 4 cm and the substrate was deposited at room temperature. Thin GST-124 films were deposited on Si substrates and then were annealed from 100 to 400°C temperatures in vacuum with heating rate of 5°C/min.

The X-ray diffraction (XRD) scans were performed using a Shimadzu model 6000 diffractometer, operating at a wavelength of 1.5418A (Cu Kα radiation, 40 kV, 30 mA), under the grazing incidence angle (θ) of 1 degree and 2θ of 20-50 degrees. The surface topography of deposited and annealed films was investigated by atomic force microscopy (AFM) in non-contact operating mode using a Park XE-100 equipment (silicon tip with conical shape) with a roughness resolution of 0.1nm.

Raman spectra were recorded at room temperature by confocal Raman microscope (Renishaw) equipped with a laser of 532nm and a Leica DM2500 microscope. The single beam power of the laser was 50mW with 100%.

The EDX spectra were taken by the ultra-high resolution scanning electron microscope Hitachi SU8010 instrument. The microscope is equipped with Oxford EDXS unit capable to determine elements down to Be.

3. Results

The thin film with a thickness of 120 nm was deposited in amorphous structure. The X-ray diffraction technique was applied to obtain information about crystallization of GST-124 film. In figures 1 and 2, the X-ray patterns of GST-124 film annealed in the temperature range 100-350°C are presented. In each case, the films were annealed for 20 min in vacuum.

In Fig. 2, the XRD pattern of the sample annealed to 200°C for a comparison with film samples annealed at higher temperature is presented.

The film surface roughness is important for the performance of the device since the electrical properties depend on the microstructure of the film-electrodes interface. In the figures 3a-e, the images of the surface topography of annealed thin film were obtained using the AFM method. The film surface roughness measurements have been done for the annealed sample which presents a clear transformation of film structure.

The Raman spectra of GST-124 film at various annealing temperatures and the EDX spectrum of thin film at 200°C are presented in Figs. 4 and 5.

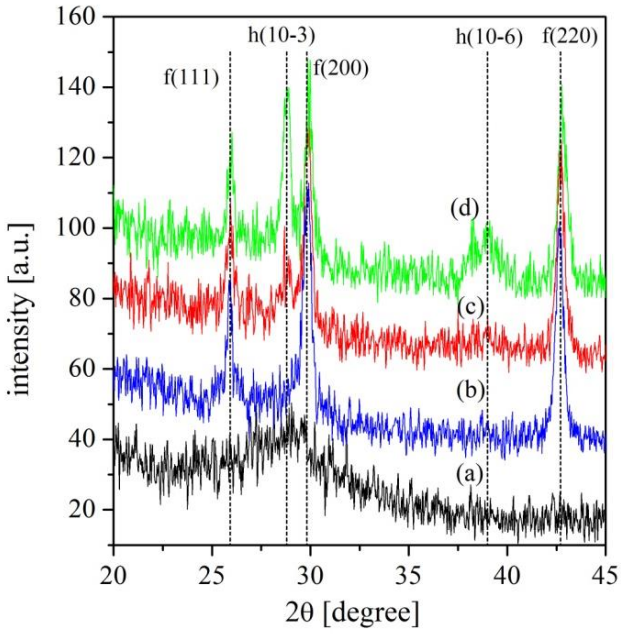

Fig. 1. The X-ray pattern of GST-124 film, a) annealing temperature T = 100°C, b) T=150°C, c) T = 175°C, d) T = 200°C

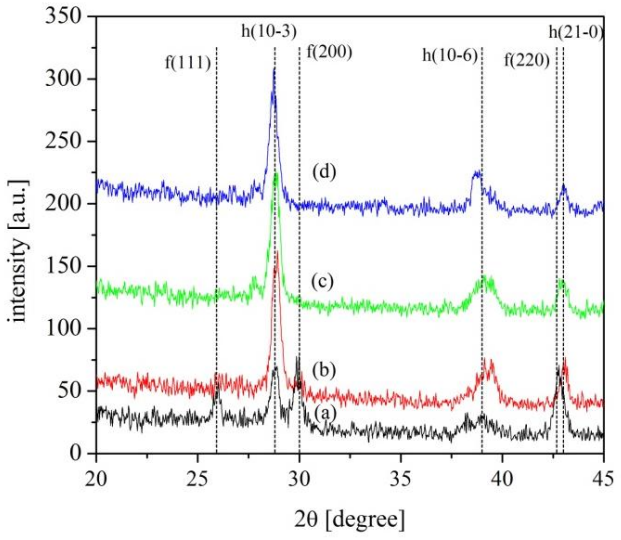

Fig. 2. The X-ray pattern of GST-124 film, a) annealed temperature T = 200°C, b) T = 225°C, c) T = 275°C and d) T = 350°C

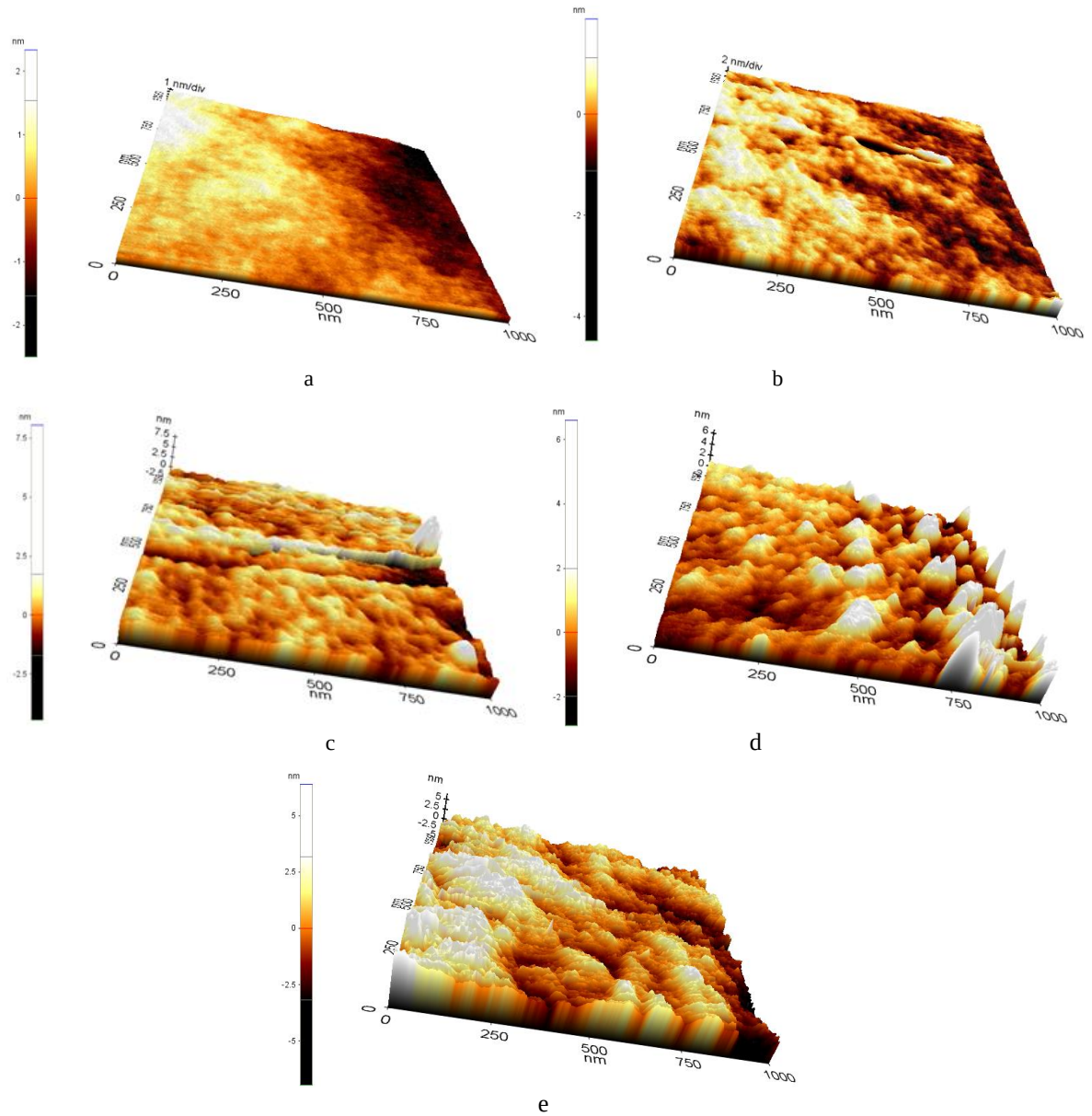

Fig. 3. a) AFM image after annealing GST-124 film at T = 100°C; b) T = 150°C, c) T = 175°C, d) T = 200°C, e) T = 350°C

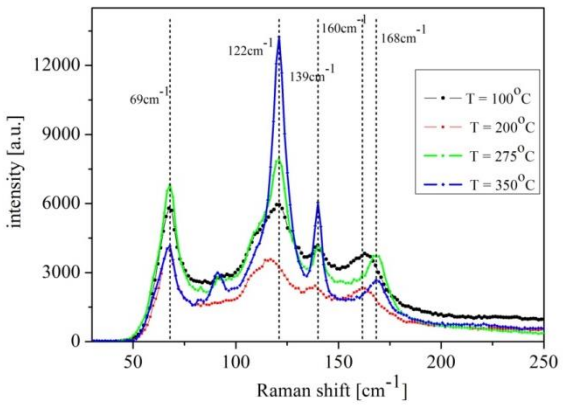

Fig. 4. The Raman spectra of GST-124 films on Si substrate at various annealing temperatures a) black curve T = 100°C, b) red curve T = 200°C, c) green curve T = 275°C and d) blue curve T =350°C

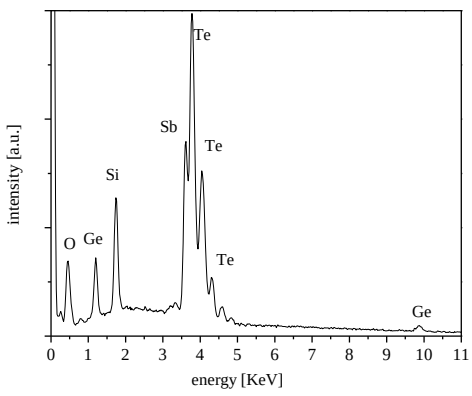

Fig. 5. The EDX spectrum of GST-124 deposited on a Si substrate at annealing temperature of 200°C

4. Discussion

In Fig. 1, the GST-124 films annealed in the temperature range of 100-150^{o}C show a crystalline metastable phase, face cubic centred (fcc), and the film annealed at temperature 100^{o}C has a minor amorphous phase with a broad and weak peak originating between 26^{o} and 29^{o}. The metastable phase fcc of GST-124 film presents the main diffraction peaks, (200) at 29.8 degree, (220) at 42 degree, respectively, and a small peak (111) at 25.9 degree. From Figs. 1 and 2, in the temperature range of 175-225^{o}C, the GST-124 films show a mixing between fcc and hexagonal closed packed (hcp) phases, and increasing the annealing temperature higher than 225^{o}C the metastable fcc structure has been fully transformed to the more stable hexagonal structure.

The stable hcp structure presents three peaks, (10-3) at 28.8 degree, (10-6) at 39 degree and (21-0) at 43 degree, respectively. By means of X-ray diffraction measurements could be observed that the first transition temperature between amorphous and fcc phases is near to 150^{o}C, close to the value reported previously [18], and the second transition temperature from fcc to hcp is close to 225^{o}C, probably even smaller. Compared to most common used $Ge_2Sb_2Te_5$, the GST-124 film used here show low second transition temperature, possibly due to vacancies of its structure.

In the Fig. 3a-d, the surface topography of GST-124 films is presented. The route-mean-square surface roughness of the GST-124 film are a) R = 0.381nm, b) R = 0.571nm, c) R = 0.881nm, d) R = 1.013nm and e) R = 1.619nm, respectively. At low annealing temperatures at 100 and 175^{o}C, the roughness of GST-124 film is quite small, but as the annealing temperature is increased, the roughness of the surface shows an increase. The error of roughness measurements was 0.1nm. The crystallization of the material surface samples close to fcc/hcp transition phases leads to an appreciable increase of the roughness. The annealed films had relatively uniform surfaces but at high temperature many crystallites had grown on the surface films, the crystallites grains increased as the annealing temperature is increasing. For film annealed at temperature of 350^{o}C the roughness reached a value of 1.619nm. In the same time at annealing temperature, T=350^{o}C, a better compactness of the surface is observed.

The local structure of the as-deposited and crystalline GST-124 films was determined on the basis of Raman scattering spectroscopy presented in figure 4. The main feature of the Raman spectra was taken in the range of 50-250cm^{-1}, and four phonon vibration modes at ~69, ~122, ~139 cm$^{-1,}$ and 160 cm^{-1}, respectively, are presented being in good agreement with the work *H.R. Yoon et al.*[6]. The Raman spectra of the present work do not match with those presented in reference 23, where these bands are located at 110 and 160 cm^{-1} in cubic $Ge_2Sb_2Te_5$ and at 129 and 152 cm^{-1} in amorphous Ge2Sb2Te5, these bands being assigned to vibrations of defective octahedra. According to our results, two broad peaks of GST-124 film annealed at temperatures 100 and 200^{o}C are observed around ~122cm^{-1} and ~160-168cm^{-1}, respectively, regarded to the main features of Raman spectra of amorphous and crystalline phases. The most intense peak with maxima at ~120–125 cm^{-1} and the peak at 139 cm^{-1}, can be related to $\Gamma_1(A_1)$ mode of $GeTe_{4-n}Ge_n$(n= 1, 2) corner-sharing tetrahedral according to the assignment in the amorphous GeTe layers [24,25].

The A_1g(2) Raman-active mode of crystalline GST-124 is presented to 166-168 cm^{-1}, at temperature ranges of 150-350^{o}C, this mode is assigned to the Sb_2Te_3 vibration [20]. In some studies [24,25], the presence of Te-Te mode at 150cm^{-1} exists mainly in amorphous GST, but in our work, the presence of Raman band at 150cm^{-1} is not observed, even at temperature of 100^{o}C for the amorphous GST spectra presented in figure 4.

A possible explanation of the lack of mode at 150cm^{-1} is given in *Nemec et al.*, that the Te-Te bond is vibrations is likely improbable, since according to EXAFS data analysis and high energy XRD and neutron experiments reveals no homopolar Te-Te bonds in GST-225 [26-28].

In addition, according to reference [25] and following the arguments of reference [20] by *Nemec et al.* since Te-Te bonds require a formation of anti-site defects, and the enthalpy formation is high [1.2 eV for exchanging the positions of one atom of Te and Sb), the Te-Te bonds are unlikely to occur in the crystalline phase. However, taking into account our XRD measurements it can be seen that at low temperature of 150^{o}C the GST-124 films presents a crystalline fcc phase. The Raman spectrum from Fig. 4 shows a mode with maxima at ~90 cm^{-1} at temperature of 350^{o}C. This mode is attributed to the Γ3 (E) mode in single-crystalline α-GeTe[20].

The qualitative chemical composition of the films, which was measured by EDX in atomic percentages, is shown in Fig. 5. The characteristic x-ray lines from Ge, Sb, and Te have been detected such as Ge 11,42%, Sb 30,7%, Te 49,9% and O 8,28%. Considering the experimental error of the EDX method of 2%, the atomic composition of the films on Si substrates is slightly over stoichiometric in Sb content.

5. Conclusion

The $Ge_1Sb_2Te_4$ phase-change thin film has been deposited by PLD at room temperature. Phase transitions from the amorphous to fcc and further to stable hcp structures occurred at temperature of 150 and 225^{o}C, respectively. The first transition temperature amorphous-fcc is similar to that obtained by previous methods.

The AFM surface topography of samples have relatively uniform surface. The roughness of films increased with the annealing temperature close to hexagonal structure. A higher roughness and good compactness of samples is observed for annealing temperature at 350^{o}C.

By Raman spectroscopy measurements phonon modes $Ge_1Sb_2Te_4$ films were detected and at high temperature the modes became sharp indicating good film crystalline

properties. The atomic composition of the $Ge_1Sb_2Te_4$ films presented a slightly over stoichiometric in Sb content.

Acknowledgements

The work was partly supported by Project PNII 174/2012.

References

[1] H. Kado, T. Tohda, Japanese Journal of Applied Physics **36,** 523 (1997).
[2] M. A. Popescu, Journal of Ovonic Research **1**, 69 (2005).
[3] M. A Popescu, Journal of Ovonic Research **2**(4), 45 (2006).
[4] M. S. Iovu, E. P. Colomeico, V. G. Benea, M. Popescu, A. Lorinczi, A. Velea, J. Optoelectron. Adv. M. **13,** 1483 (2011).
[5] K. Sugawara, T. Gotoh, K. Tanaka, Applied Physics Letters **79**(10), 1549 (2001).
[6] H. R. Yoon, W. Jo, E. Cho, S. Yoon, M. Kim, Journal of Non-Crystalline Solids **352**, 3757 (2006).
[7] S. Lay, T. Lowrey, OUM - A 180 nm nonvolatile memory cell element technology forstand alone and embedded applications, IEDM Tech. Dig. (2001) 803.
[8] S. J. Hudgens, OUM Non-volatile Semiconductor Memory Technology Overview, Mater. Res. Soc. Symp. Proc. Vol. 9180918-H05-01-G06-01 (2006).
[9] S. R. Ovshinski, Physics Review Letters **21,** 1450 (1968).
[10] M. Wuttig, D. Lusebrink, D. Wamwangi, W. Wenic, M. Gillessen, R. Dronskowski, Nature Materials **6,** 122 (2007).
[11] S. Hosokawa, T. Ozaki, K. Hayashi, N. Happo, M. Fujiwara, K. Horii, P. Fons, A. V. Kolobov, J. Tominaga, Applied Physics Letters **90**, 131913 (2007).
[12] S. Privitera, E. Rimini, C. Bongiorno, A. Pirovano, R. Bez, Nuclear Instruments and Methods in Physics Research Section B: Beam Interactions with Materials and Atoms **257**, 352 (2007).
[13] R. De Bastiani, A. M. Piro, M. G. Grimaldi, E. Rimini, Nuclear Instruments and Methods in Physics Research Section B: Beam Interactions with Materials and Atoms **257,** 572 (2007).
[14] Y. Kim, K. Jeong, M. H. Cho, U. Hwang, H. S. Jeong, K. Kim, Applied Physics Letters **90**, 171920 (2007).
[16] F. Yan, T. J. Zhu, X. B. Zhao, S. R. Dong, Applied Physics A-Materials Science and Processing **88**, 425 (2007).
[16] D. H. Kim, M. S. Kim, R. Y. Kim, K.S. Kim, H. G. Kim, Materials Characterization **58,** 479 (2007).
[17] E. Morales-Sanchez, E. F. Prokhorov, J. Gonzales-Hernandez, A. Mendoza-Galván, Thin Solid Films **471,** 243 (2005).
[18] M. Osiac, V. Tiron, G. E. Iacobescu, G. Popa, Dig J Nanomater Bios **9**, 451 (2014).
[19] H. Lu, E. Thelander, J. W. Gerlach, D. Hirsch, U. Decker, B. Rauschenbach, Applied Physics Letters **101**, 031905 (2012).
[20] P. Nemec, V. Nazabal, A. Moreac, J. Gutwirth, L. Benes, M. Frumar, Chemistry and Physics **136,** 935 (2012).
[21] M. Bouška, S. Pechev, Q. Simon, R. Boidin, V. Nazabal, J. Gutwirth, E. Baudet, P. Němec, Scientific Reports **6,** 26552 (2016).
[22] H. Lu , E. Thelander, J. W. Gerlach, U. Decker, B. Zhu, B. Rauschenbach, Adv. Funct. Mater. **2,** 3621 (2013).
[23] G. C. Sosso, S. Caravati, R. Mazzarello, M. Bernasconi, Phys. Rev. **B83**, 134201 (2011).
[24] K. S. Andrikopoulos, S. N. Yannopoulos, A. V. Kolobov, P. Fons, J. Tominaga, Journal of Physics and Chemistry of Solids **68**, 1074 (2007).
[25] Wen-Pin Hsieh, Peter Zalden, Matthias Wuttig, Aaron M. Lindenberg, Wendy L. Mao, Applied Physics Letters **103,** 191908 (2013).
[26] D. A. Baker, M. A. Paesler, G. Lucovsky, S. C. Agarwal, P. C. Taylor, Phys. Rev. Lett. **96,** 255501 (2006).
[27] G. Lucovsky, D. A. Baker, M. A. Paesler, J. C. Phillips, J. of Non-crys Solid **353,** 1713 (2007).
[28] P. Jovari, I. Kaban, J. Steiner, B. Beuneu, A. Schops, A. Webb, J. Phys.: Condens. Matter **19,** 335212 (2007).

*Corresponding author: m_osiac@yahoo.com